Efficient Data Acquisition for MR Doppler

D. Lee[1], A. B. Kerr[1], J. M. Santos[1], B. S-C. Hu[2], and J. M. Pauly[1]

[1]Electrical Engineering, Stanford University, Stanford, California, United States, [2]Palo Alto Medical Foundation, Palo Alto, California, United States

INTRODUCTION: MR Doppler is a technique that provides real-time imaging of the velocity profile of blood flow analogous to Doppler ultrasound imaging. It provides a mechanism for quickly interrogating valvular flow characteristics, either for identifying valvular stenoses or regurgitant flow [1-3]. To detect peak velocity of patients, velocity field of view (FOV_v) is often required to be in the range ±4m/s, which results in a lower spatial resolution compared to when small FOV_v is sufficient. This is because small change in M_1 (1st moment of gradient) comes with small change in M_0 (0th moment of gradient) for time-optimal bipolar waveforms. As suggested in Ref. 4, we can achieve higher spatial resolution by traversing circular *k*-space. We present a flexible design method that makes it easier to realize the desired *k*-space trajectory in a time-optimal way.

THEORY: Even though it is easy to achieve a circular boundary shape with a simple tweaking approach [4], it is not ideal in the sense that the trajectory is defined at the boundary since we normally define the density along the k_v axis where $k_z = 0$. Thus, we want to directly prescribe the points to be traversed in *k*-space, which turns this problem into a traversal through multi-points in *k*-space while preserving the overall time-optimality. Rather than formulating this as an optimization problem, we decompose it into sub-sections such that the combined waveform does not lose the time-optimality. After breaking the acquisition trajectory into separate sections, we separately design time-optimal gradient waveforms using a multidimensional time-optimal gradient design method [5] with which waveform design becomes a simple function denoted as **mtg**(·). Then, the resultant gradient waveform is a sum of sub-waveforms.

$$g(t)=\sum_{k=0}^{K} g^k(t) \quad where \quad g^k(t)=\mathbf{mtg}(t_i^k, g_i^k, g_f^k, \Delta M_0^k, \Delta M_1^k)$$

g_i^k, g_f^k : initial and final value of $g^k(t)$, which starts at t_i^k

$\Delta M_0^k, \Delta M_1^k$: desired 0th, 1st moment change by $g^k(t)$

Figure 1 illustrates the advantage of the sub-problem approach over conventional bipolar waveform design. It avoids tuning process which is a practical way of compensating the ΔM_1 offset introduced by the prewinder which adjusts whole *k*-space ROI. Even though we design a bipolar gradient satisfying $\Delta M_1(t_c,t_a)$, what we really want to achieve is $\Delta M_1(t_d,t_b)$. Thus, we have to iteratively adjust the value of $\Delta M_1(t_c,t_a)$ to have $\Delta M_1(t_d,t_b)$ meet the requirement. By breaking the bipolar waveform into 3 parts (a⇀b, b⇀d', d'⇀d), we can directly generate the overall waveform by concatenating 3 sub-waveforms. The conventional iterative approach is more troublesome when designing variable density trajectory where iterative adjustment should be performed for every spoke. The new approach reduces the pulse duration by merging the prewinder with the 1st spoke (similarly, the last spoke and the rewinder). Note that $g^k(t)$ must be calculated in the proper order to achieve time optimality. For example, we want to decide the section d'⇀d before b⇀d' for the sake of time-optimality. This corresponds to calculating $g^{1,f}(t)$ after $g^{1,b}(t)$ in Fig. 2.

METHODS: Designs were constrained by gradients of 40 mT/m maximum amplitude and 150 T/m/s maximum slew rate (GE 1.5T Signa scanner). Waveforms of 16ms readout with 4m/s FOV_v were used for imaging at the aortic valve using a real-time system [6]. The *k*-space data were gridded and multiplied by a Hamming window while applying homodyne partial *k*-space reconstruction.

RESULTS AND DISCUSSION: We could achieve higher spatial resolution in each space-velocity image at the aortic valve as shown in Fig. 3 without harming the ability of resolving the velocity spectrum in the velocity dimension. This is applicable to other variations like variable-density [3] and interleaved approach [7] to achieve higher resolution in velocity since we can accurately prescribe and realize the *k*-space required by these methods.

REFERENCES: [1] Irarrazabal, P et al., *Magn. Reson. Med.*, 30:207-212 (1993) [2] MacGowan, CK et al., *J. Magn. Reson. Imag.*, 21:297-304 (2005) [3] DiCarlo, JC et al., *Magn. Reson. Med.*, 54:645-655 (2005) [4] Lee, D et al., *ISMRM* 15th, 2549 (2007) [5] Hargreaves, BA et al., *Magn. Reson. Med.*, 51:81-92 (2004) [6] Santos, JM et al., *IEEE EMBS* 26th, 1048-1051 (2004) [7] Kerr, AB et al., *SCMR* 10th, p647 (2007)

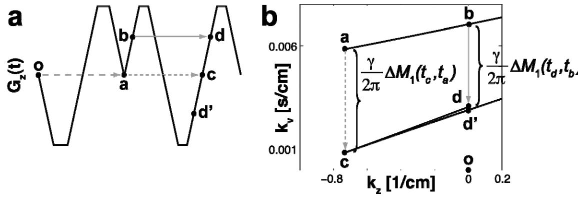

Figure 1. ΔM_1 offset introduced by the prewinder on the basic bipolar waveform. (a) Gradient waveform of prewinder and the 1st main lobe (b) *k*-space trajectory for the sub-section, a ⇀ d

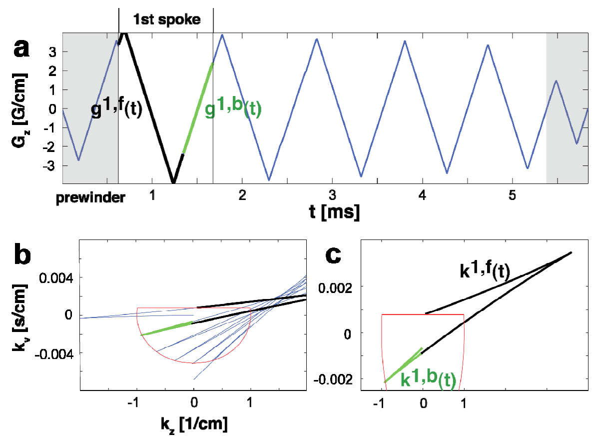

Figure 2. Depiction of the time-optimal gradient waveform design method (FOV_v = 6m/s, Δv = 1m/s, Δz = 0.5cm/s). (a) gradient waveform (b) trajectory in *k*-space (c) close-up of the 1st spoke

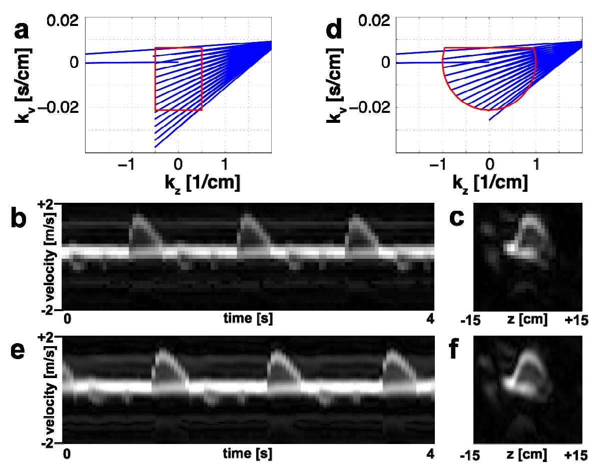

Figure 3. Comparison of in vivo images (FOV_v = 4m/s). (a~c) rectangular ROI in *k*-space, Δz = 1.0cm (d~f) circular ROI in *k*-space, Δz = 0.5cm (a,d) *k*-space trajectories (b,e) time-velocity images (c,f) space-velocity images at systole.